P-waves from cross-correlation of seismic noise

Philippe Roux, Karim G. Sabra, Peter Gerstoft, and W. A. Kuperman
Marine Physical Laboratory, University of California San Diego, La Jolla, California, USA

Michael C. Fehler
Los Alamos National Laboratory, Los Alamos, New Mexico, USA

[1] We present results from the cross-correlations of seismic noise recordings among pairs of stations in the Parkfield network, California. When performed on many station pairs at short ranges, the noise correlation function (NCF) is the passive analog to a shot gather made with active sources. We demonstrate the presence of both a P-wave and a Rayleigh wave in the NCF. A time-frequency analysis allows us to separate the two wave packets that are further identified through their polarization. Arrival times were estimated from the NCF and they compared favorably with predictions using ray tracing in a regional velocity model and with the velocity gradient across the San Andreas Fault. **Citation:** Roux, P., K. G. Sabra, P. Gerstoft, W. A. Kuperman, and M. C. Fehler (2005), P-waves from cross-correlation of seismic noise, *Geophys. Res. Lett.*, *32*, L19303, doi:10.1029/2005GL023803.

1. Introduction

[2] Cross-correlation of noise recordings can be used to infer the impulse response between receivers. Extensive work has been performed on this topic in the past few years in various fields of wave physics such as ultrasonics [*Weaver and Lobkis*, 2001, 2004], underwater acoustics [*Roux et al.*, 2004] and geophysics [*Rickett and Claerbout*, 1999; *Campillo and Paul*, 2003; *Shapiro and Campillo*, 2004; *Wapenaar*, 2004; *Sabra et al.*, 2005a; *Shapiro et al.*, 2005]. Despite the very different scales involved in ultrasonics (wavelength $\sim$ mm) compared to geophysics (wavelength $\sim$ km), the basic physics of the process is the same. The impulse response between two receivers is derived from the part of the noise that remains coherent between them, even if, at first inspection, it is deeply buried into local incoherent noise. After cross correlating over a long time (for example, one month in [*Sabra et al.*, 2005a; *Shapiro et al.*, 2005]), the noise correlation function (NCF) converges to the impulse response between the two receivers filtered by the bandwidth of the noise spectrum.

[3] The convergence of the NCF to the impulse response is strongly influenced by the variations in the spatial distribution of the noise sources and the spectral content of the noise recordings. The noise spectrum defines the frequency bandwidth over which the impulse response can be retrieved. When receivers are widely separated, the coherent propagating noise must have sufficient amplitude to be recorded on both receivers despite geometrical spreading and attenuation. This explains why the slowly-attenuated

Rayleigh waves have dominated the impulse response obtained so far from correlation of seismic noise. The spatial distribution of seismic noise is also of importance. When noise sources are uniformly distributed on both sides of the receivers, the correlation function is symmetric in time, showing both the impulse response and its time-reverse [*Snieder*, 2004; *Roux et al.*, 2005]. However, recent papers focused on noise data recorded in Southern California and did not result in a symmetric NCF because the noise was dominated by microseism originating from the ocean [*Sabra et al.*, 2005a; *Shapiro et al.*, 2005].

[4] The aim of this paper is to show that P-waves can also be extracted from closely-spaced receivers (less than 11 km) from the correlation of seismic noise.

2. Data Processing and Experimental Results

[5] To demonstrate that P-waves can be extracted from seismic noise data, we processed data recorded on the dense temporary seismic network installed in the Parkfield area between July 2001 and October 2002 [*Thurber et al.*, 2004]. One month of seismic noise data were cross-correlated between each pair of 30 broadband 3-component seismic stations located in an 11-km square (Figure 1a). This network has been extensively used to monitor and image the San Andreas Fault (SAF) using both man-made explosions and earthquakes. Inversion results have confirmed the spatial heterogeneity of P-wave velocity across the Fault up to 6 km in depth [*Ben-Zion and Malin*, 1991; *Catchings et al.*, 2002; *Thurber et al.*, 2004]. The correlation process is used to show that P-waves (and not only Rayleigh waves) are also extracted at short distances from seismic noise recordings.

[6] The processing performed on 1-day noise recording on one seismometer consists of: 1) eliminating high-amplitude events by truncating the recording amplitude at three times the standard deviation of the ambient noise signal; 2) equalization of the noise spectrum in the frequency interval $0.1-1.3$ Hz. The purpose of this processing is to homogenize the noise signal over the frequency interval for which coherent seismic noise is still present (which had an upper limit of about 1.3 Hz).

[7] Plane wave beamforming is then applied to the processed noise traces to measure the angular distribution of noise (Figure 1b). As observed before [*Sabra et al.*, 2005b; *Shapiro and Campillo*, 2004], the noise comes mainly from the Pacific Ocean in the frequency interval of interest. Previous work has shown that the NCF obtained using noise having a spatial distribution with a predominant propagation direction converges to a one-sided impulse
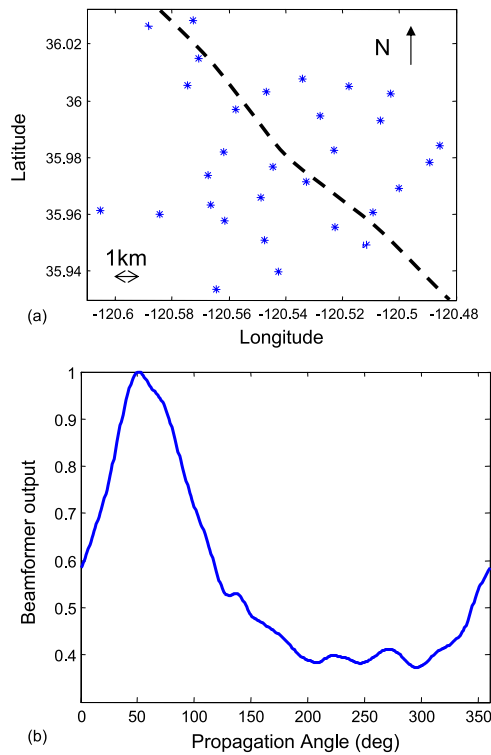
Figure 1. (a) Map of the Parkfield area (an 11-km large square), showing stations (*) and SAF (dashed). (b) Angular distribution of incoming noise on the Parkfield network averaged over one month. Plane wave beamforming is summed incoherently over 70 frequencies from 0.1–1.3 Hz (North is 0°).

response between pairs of stations [*Roux et al.*, 2004]. The directivity angle depends on the frequency and the range between the station pair.

[8] Among the 30 stations analyzed, all 146 station pairs whose relative locations lie along lines having azimuths between 40°–60° have been selected. This range of azimuths was chosen to include the main noise propagation direction from Figure 1b. Figure 2a shows the spatial-temporal correlation function for the Z-Z components of the noise field and reveals the presence of fast and slow waves propagating at about 5 and 2 km/s, respectively. Figure 2a is the passive analog of the shot gathers obtained during the seismic reflection/refraction survey conducted by *Catchings et al.* [2002]. In Figures 2b and 2c, the spatial-temporal NCF has been filtered in two different frequency bands, which show that the fast and slow waves travel at high and low frequency, respectively.

[9] Both the Z-Z and Z-R traces obtained from the NCF for two stations separated by 8.8 km are displayed in Figure 3a. Each trace is normalized by the noise auto-correlation at each station so that the amplitude of the NCF is representative of the coherence of the noise field between the two stations. Figure 3b corresponds to a time-frequency analysis of the Z-Z component of the NCF. Two wave packets are distinguishable at high (0.9 Hz) and low (0.4 Hz) frequencies. The low frequency wave packet is dispersive as expected for a Rayleigh wave. The observed dispersion fits well with the dispersion computed from the red velocity

profile in Figure 4a (assuming Vp/Vs ~ √3). Figures 3c and 3d show the polarization plots for these two wave packets. The linear particle motion obtained at 0.9 Hz indicates the presence of a P-wave while the elliptical particle motion obtained at 0.4 Hz is a further evidence of a Rayleigh wave.

[10] Figure 4 shows ray paths for the P-wave performed in a simplified 1-D seismic-velocity model of the SAF [*Catchings et al.*, 2002; *Thurber et al.*, 2004]. The ray arrival inclination at range 8.8 km matches the polarization angle Θ (Figure 3c) obtained from the NCF. This polarization behavior for station pairs from 6 to 11 km apart, is consistent with the ray-modeled inclination varying from 60° to 70° (Figure 4b) and with the observed inclination
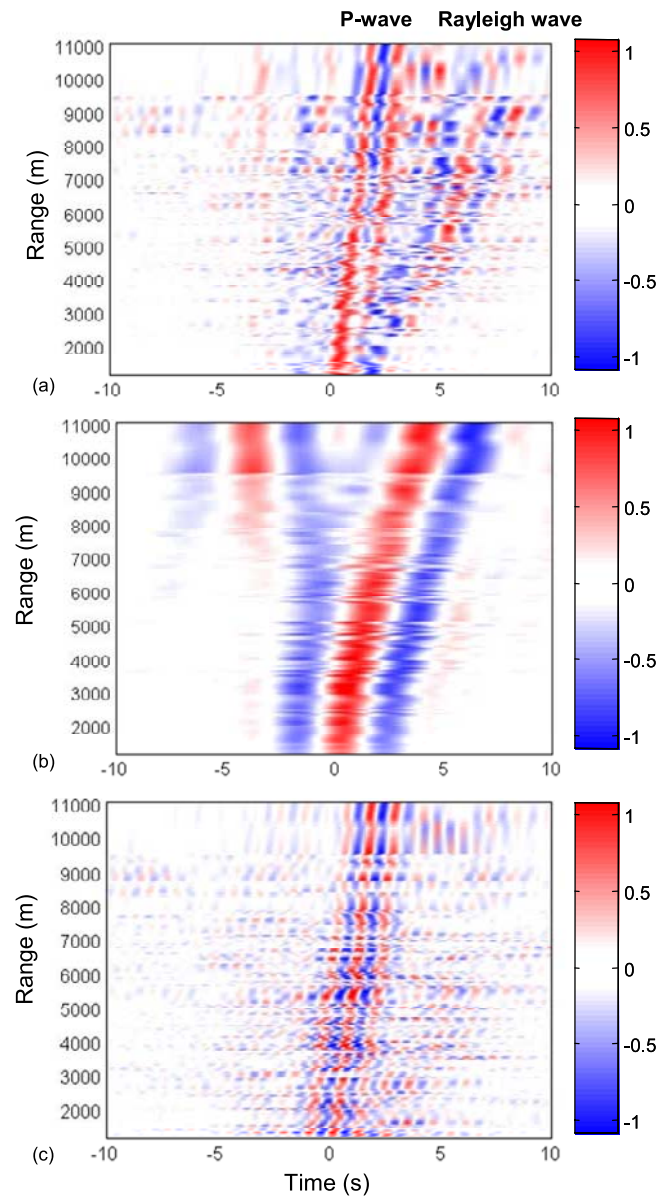

Figure 2. Range-time representation of the Z-Z component of the noise correlation tensor averaged over one month in three frequency bands (a) [0.1–1.3 Hz], (b) [0.1–0.45 Hz], and (c) [0.7–1.3 Hz]. Each plot has been normalized by its own maximum.

from the P-wave polarization which was always greater than 60°, after correcting for the free surface reflection [*Kennett*, 2002].

3. Discussion and Conclusions

[11] Previous studies using seismic noise recorded by stations separated by larger distances (30−500 km) showed that the NCF was dominated by Rayleigh waves [*Sabra et al.*, 2005b; *Shapiro and Campillo*, 2004], indicating that noise propagates mainly as surface waves [*Aki and Richards*, 1980]. One may speculate what process gives birth to P-waves at short range. P-waves may be created by local man-made sources, but these are not the main component of seismic noise. Most microseism energy propagates as Rayleigh waves [*Aki and Richards*, 1980] and likely a fraction of this energy is locally converted into body waves because of heterogeneities in the Earth's upper crust. Once generated, P-waves propagate above a cutoff frequency, which can be approximately determined using the WKBJ approximation [*Aki and Richards*, 1980] as c_t/L, where L is the horizontal length of the refractive path and c_t is the P-velocity at the turning point (at 8.8 km we obtain 0.6 Hz in agreement with the 0.65 Hz observed in Figure 3b). Lastly, P-waves will attenuate faster than Rayleigh waves because of larger geometric loss (spherical versus cylindrical) and longer path length (Figure 4b).

[12] Finally, Figure 4c shows the estimated travel time for the P-wave as determined by the maximum of the time derivative of the NCF [*Roux et al.*, 2004; *Sabra et al.*, 2005a]. We observe that P-waves propagate faster on the west side than on the east side of the SAF, in agreement with the strong P-wave velocity contrast across the SAF in the Parkfield area [*Ben-Zion and Malin*, 1991; *Eberhart-*

Figure 4. (a) P-wave velocity profiles deduced from previous tomography modeling (blue) and based on fitting the dispersion curve in Figure 3c (red). Bounds of the velocity profiles (dashed) are determined based on *Catchings et al.* [2002]. (b) Ray tracing showing P-wave refraction from different launch angles using a 1-D velocity profile (blue in a). (c) Comparison between the P-wave travel times obtained from the time-derivative of the NCF for 111 station pairs and the prediction of the ray code (blue) from the P-wave velocity profile (blue in a). The green circles and red stars correspond to station pairs located on the east or west sides of the SAF, respectively, while black crosses are station pairs located on each side of the SAF. The dashed lines correspond to maximum and minimum arrival times obtained from a Monte Carlo simulation using velocity profiles generated from within the velocity bounds in (a).

Phillips and Michael, 1993; *Thurber et al.*, 2004]. The increase in apparent P-wave velocity, as evidenced by the slope change for the time-distance plot, is consistent with a P-wave model having increasing velocity with depth. Despite conclusive work at large ranges (∼30−600 km) using Rayleigh waves for constructing surface velocity maps [*Shapiro et al.*, 2005; *Sabra et al.*, 2005b], tomography inversion at such short ranges from seismic noise data using both surface and body waves remains to be demonstrated.
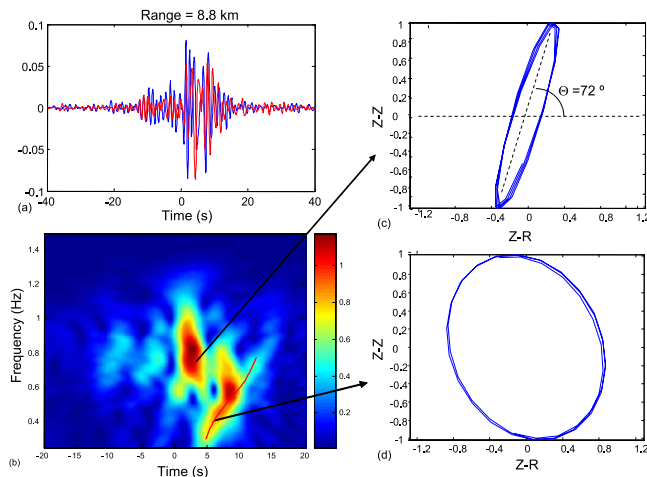
Figure 3. (a) Z-Z (blue) and Z-R (red) traces of the noise correlation function averaged over one month for a station pair separated by 8.8 km. (b) Frequency-time analysis of the Z-Z component of the noise correlation function shown in (a). In red is plotted the dispersion curve for the Rayleigh wave using the red velocity profile in Figure 4a. (c) Polarization of the high-frequency wave obtained at 0.9 Hz from the particle motion plots of the Z-Z versus Z-R components of the noise correlation tensor in the time-window [0−4.5s]. (d) Same as (c) for the low-frequency wave at 0.4 Hz in the time-window [4.5−9s].
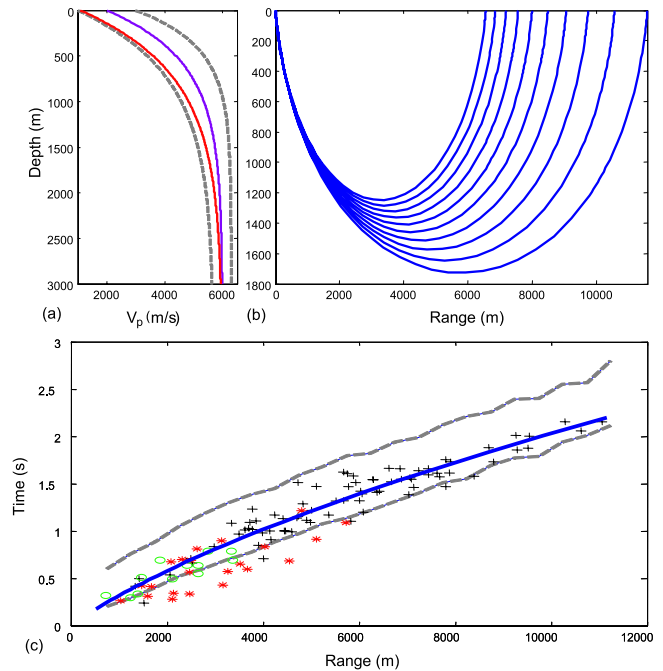
References

Aki, K., and P. G. Richards (1980), *Quantitative Seismology: Theory and Practice*, pp. 487−498, W. H. Freeman, New York.
Ben-Zion, Y., and P. Malin (1991), San Andreas Fault zone head waves near Parkfield, California, *Science*, *251*, 1592−1594.
Campillo, M., and A. Paul (2003), Long-range correlations in the diffuse seismic coda, *Science*, *299*, 547−549.
Catchings, R. D., M. J. Rymer, M. R. Goldman, J. A. Hole, R. Huggins, and C. Lippus (2002), High-resolution seismic velocities and shallow struc-

ture of the San Andreas fault zone at Middle Mountain, Parkfield, California, *Bull. Seismol. Soc. Am.*, *92*, 2493–2503.

Eberhart-Phillips, D., and A. J. Michael (1993), Three-dimensional velocity structure, seismicity and fault structure in the Parkfield region, central California, *J. Geophys. Res.*, *98*, 15,737–15,758.

Kennett, B. L. N. (2002), *The Seismic Wavefield*, vol. I, p. 171, Cambridge Univ. Press, New York.

Rickett, J., and J. Claerbout (1999), Acoustic daylight imaging via spectral factorization: Helioseismology and reservoir monitoring, *Leading Edge*, *18*, 957–960.

Roux, P., W. A. Kuperman, and the NPAL Group (2004), Extracting coherent wavefronts from acoustic ambient noise in the ocean, *J. Acoust. Soc. Am.*, *116*, 1995–2003.

Roux, P., K. G. Sabra, W. A. Kuperman, and A. Roux (2005), Ambient noise cross-correlation in free space: Theoretical approach, *J. Acoust. Soc. Am.*, *117*, 79–84.

Sabra, K. G., P. Gerstoft, P. Roux, W. A. Kuperman, and M. C. Fehler (2005a), Extracting time-domain Greens function estimates from ambient seismic noise, *Geophys. Res. Lett.*, *32*, L03310, doi:10.1029/2004GL021862.

Sabra, K. G., P. Gerstoft, P. Roux, W. A. Kuperman, and M. C. Fehler (2005b), Surface wave tomography from microseism in Southern California, *Geophys. Res. Lett.*, *32*, L14311, doi:10.1029/2005GL023155.

Shapiro, N. M., and M. Campillo (2004), Emergence of broadband Rayleigh waves from correlations of the ambient seismic noise, *Geophys. Res. Lett.*, *31*, L07614, doi:10.1029/2004GL019491.

Shapiro, N. M., M. Campillo, L. Stehly, and M. H. Ritzwoller (2005), High-resolution surface wave tomography from ambient seismic noise, *Science*, *307*, 1615–1617.

Snieder, R. (2004), Extracting the Green's function from the correlation of coda waves: A derivation based on stationary phase, *Phys. Rev. E*, *69*, 046610.

Thurber, C., S. Roecker, H. Zhang, S. Baher, and W. Ellsworth (2004), Fine-scale structure of the San Andreas Fault zone and location of the SAFOD target earthquakes, *Geophys. Res. Lett.*, *31*, L12S02, doi:10.1029/2003GL019398.

Wapenaar, K. (2004), Retrieving the elastodynamic Green's function of an arbitrary inhomogeneous medium by cross correlation, *Phys. Rev. Lett.*, *93*, 254301.

Weaver, R. L., and O. I. Lobkis (2001), Ultrasonics without a source: Thermal fluctuation correlations at MHz frequencies, *Phys. Rev. Lett.*, *87*, 134301.

Weaver, R. L., and O. I. Lobkis (2004), Diffuse fields in open systems and the emergence of the Green's function, *J. Acoust. Soc. Am.*, *116*, 2731–2734.

————————————

M. C. Fehler, Los Alamos National Laboratory, Los Alamos, NM 87545, USA.

P. Gerstoft, W. A. Kuperman, P. Roux, and K. G. Sabra, Marine Physical Laboratory, University of California San Diego, La Jolla, CA 92093-0238, USA. (ksabra@ucsd.edu)